PHYSICAL REVIEW LETTERS

Effect of Poisson Ratio on Cellular Structure Formation

I. B. Bischofs and U. S. Schwarz

University of Heidelberg, Im Neuenheimer Feld 293, D-69120 Heidelberg, Germany
and Max Planck Institute of Colloids and Interfaces, D-14424 Potsdam, Germany

Mechanically active cells in soft media act as force dipoles. The resulting elastic interactions are long ranged and favor the formation of strings. We show analytically that due to screening, the effective interaction between strings decays exponentially, with a decay length determined only by geometry. Both for disordered and ordered arrangements of cells, we predict novel phase transitions from paraelastic to ferroelastic and antiferroelastic phases as a function of the Poisson ratio.

Predicting structure formation and phase behavior from the microscopic interaction laws is a formidable task in statistical mechanics, especially if the interaction laws are long ranged or anisotropic. In biological systems, the situation is further complicated because interacting components are active in the sense that informed by internal instructions (e.g., genetic programs for cells) and fueled by energy reservoirs (e.g., ATP), they react to input signals in a complicated way, which usually does not follow from an energy functional. Therefore these systems are often described by stochastic equations [1,2]. One drawback of this approach is that typically the stochastic equations have to be analyzed by numerical rather than analytical methods. However, for specific systems structure formation of active particles can be predicted from extremum principles. In this case, analytical progress might become feasible again, in particular, if analogies exist to classical systems of passive particles. One example of this kind might be hydrodynamic interactions of active particles like swimming bacteria [3]. Here this is demonstrated for another example, namely, mechanically active cells interacting through their elastic environment [4,5].

Our starting point is the observation that generation and propagation of elastic fields for active particles proceed in a similar way as they do for passive particles like defects in a host crystal, e.g., hydrogen in metal [6,7]. For a local force distribution in the absence of external fields, the overall force (monopole) applied to the elastic medium vanishes due to Newton's third law [8]. Therefore each particle is characterized in leading order of a multipolar expansion by a force dipole tensor P_{ij}. For many situations of interest, including cells in soft media, this force dipole will be anisotropic and can be written as $P_{ij} = Pn_i n_j$, where $\vec{n}$ is the unit vector describing particle orientation and P is the force dipolar moment. The perturbation of the surrounding medium resulting from a force dipole P'_{kl} positioned at $\vec{r}'$ is described by the strain tensor $u_{ij}(\vec{r}) = \partial_j \partial'_l G_{ik}(\vec{r}, \vec{r}')P'_{kl}$, where summation over repeated indices is implied and G_{ij} is the Green function for the given geometry, boundary conditions, and material properties

of the sample. The strain u_{ij} generated by one particle causes a reaction of another particle leading to elastic interactions. The essential difference between active and passive particles is that many cell types respond to strain in an opposite way as do defects. For defects the interaction with the environment leads to a linearized potential $V = -P_{ij}u_{ij}$ [6]. For example, an anisotropic defect attracting the atoms of its host lattice turns away from tensile strain, in this way enhancing the displacement fields in the medium. In contrast, for mechanically active cells like fibroblasts, experimental observations suggest that they adopt positions and orientations in such a way as to effectively minimize the scalar quantity $W = P_{ij}u_{ij} = -V$ [4,5]. For tensile strain, this implies that contractile cells actively align with the external field. Because they pull against it, they reduce displacement. For fibroblast-like cells, this behavior might have evolved in the context of wound healing, when cell traction is required to close wounds. For a translationally invariant system, the effective interaction potential between elastically interacting cells therefore follows as

$$W = P_{ij}u_{ij} = -P_{ij}\partial_j \partial_l G_{ik}(\vec{r} - \vec{r}')P'_{kl}, \qquad (1)$$

where we have used $\partial'_l G_{ik} = -\partial_l G_{ik}$. Since G scales as $\sim 1/Er$, where r is distance and E an elastic modulus, W scales as $\sim P^2/Er^3$. Otherwise the structure formation resulting from Eq. (1) strongly depends on the nontrivial angular dependance determined by G.

The simplest model for the elastic properties of the extracellular environment is isotropic linear elasticity. Thus there are two elastic constants: the Young modulus E describes the rigidity of the material and the Poisson ratio ν the relative importance of compression and shear. Its maximal value is $\nu = 1/2$ (incompressible material). If such a material is tensed in one direction, the shear mode dominates and it contracts in the perpendicular directions (*Poisson effect*). For common materials, the minimal value for the Poisson ratio is $\nu = 0$. Then the compression mode dominates and uniaxial tension does not translate into lateral contraction. Isotropic linear elasticity is a reason-

able assumption for the synthetic polymer substrates commonly used to study mechanical effects in cell culture [9,10]. In the following, we therefore use the Boussinesq Green function for particles exerting tangential forces on an elastic half-space (that is, translational invariance applies to two dimensions). Analyzing Eq. (1) then shows that W has a pronounced minimum for aligned force dipoles for all possible values of the elastic constants [4,5]. Recently, such alignment of cells in soft media has indeed been observed experimentally [11,12].

We first consider an infinitely extended string of aligned force dipoles spaced at equal distance a. An additional dipole is placed at a horizontal distance x and with a vertical offset y, compare Fig. 1. To simplify our notation, we use nondimensional quantities: energy W is rescaled with P^2/Ea^3 and length with a. Since the medium is assumed to be linear, the superposition principle applies and the effective interaction potential can be found by summing up all pairwise interactions. For parallel orientation [Fig. 1(a)], we have

$$W^{\parallel} = -\partial_y^2 \sum_{n=-\infty}^{+\infty} \left(\frac{(1-\nu)^2}{\pi[x^2+(n-y)^2]^{1/2}} + \frac{\nu(1+\nu)(n-y)^2}{\pi[x^2+(n-y)^2]^{3/2}} \right) \quad (2)$$

and for perpendicular orientation [Fig. 1(b)], we have

$$W^{\perp} = -\partial_x\partial_y \sum_{n=-\infty}^{+\infty} \frac{\nu(1+\nu)x(n-y)}{\pi[x^2+(n-y)^2]^{3/2}}. \quad (3)$$

Equations (2) and (3) can be analyzed further with methods from complex analysis. Briefly, the Poisson sum formula $\sum_{n=-\infty}^{\infty} f(in) = 1/2i \int_C dz \coth(\pi z) f(z)$ allows us to turn the sums into integrals in the complex plane [13]. By bending the contour C around suitable branch cuts introduced by the singularities of the corresponding $f(z)$ at $z = \pm x + iy$, the integral forms of Eqs. (2) and (3) can be evaluated in the limit of large x:

$$W^{\parallel/\perp} = 8\pi\nu(1+\nu)\cos(2\pi y)e^{-2\pi x}g^{\parallel/\perp}(x) \quad (4)$$

with

$$g^{\parallel}(x) = -2\pi\sqrt{x} + \frac{1}{\nu\sqrt{x}} + O(x^{-3/2}), \quad (5)$$

$$g^{\perp}(x) = 2\pi\sqrt{x} - \frac{1}{\sqrt{x}} + O(x^{-3/2}). \quad (6)$$

Thus, despite the long-ranged character of the elastic pair interaction, the effective interaction between an infinite string and a single dipole (and a second string, respectively) is short ranged and decays to leading order $\sim \sqrt{x}e^{-2\pi x}$. There is one exception, namely $\nu = 0$, when $W^{\parallel} \sim e^{-2\pi x}/\sqrt{x}$ for parallel dipoles and $W^{\perp} = 0$ for perpendicular dipoles. In dimensional units, the exponential decay occurs on a length scale $\lambda = a/2\pi$ set by the dipolar spacing a only, independent of the elastic constants. As dipole density increases, the dipolar spacing a and therefore also the screening length λ decreases.

In practice, strings will be finite. Therefore we now consider a single dipole with parallel orientation interacting with a finite string of N dipoles aligned along the y axis and centered around the origin. For simplicity, we further specify to offset $y = 0$ and Poisson ratio $\nu = 0$. For $N = 1$, the two dipoles interact via $W^{\parallel} = 1/\pi x^3$. For $N = 200$, the full interaction potential as obtained by numerical evaluation of Eq. (2) is shown as solid line in Fig. 2.
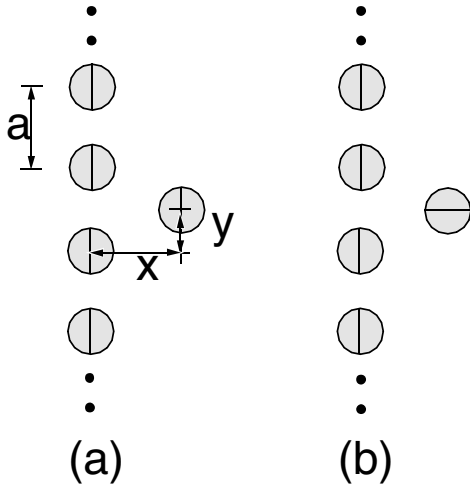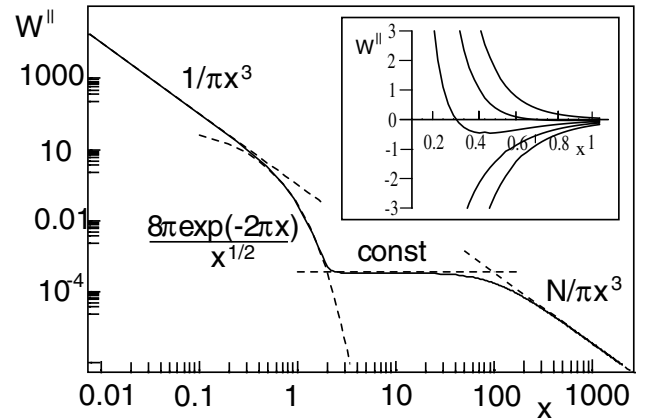

FIG. 1. Elastic interactions of cells lead to string formation. Here we consider the elastic interaction of a string of aligned dipoles spaced at equal distance a with a single additional force dipole at horizontal distance x and vertical offset y, both for (a) parallel and (b) perpendicular orientation.

FIG. 2. Interaction $W^{\parallel}$ between a finite string of N aligned dipoles and another dipole as a function of distance x for $N = 200$, offset $y = 0$ and Poisson ratio $\nu = 0$. The solid line is the numerical evaluation of Eq. (2). The dashed lines are the different scaling laws derived in the main text. Inset: $W^{\parallel}$ for an infinite string for $x < 1$, $y = 0$, and $\nu = 0, 0.2, 0.3, 0.4, 0.5$ from top to bottom.

Clearly there are different scaling regimes, which can be explained in the following way. For $x > N$, the dipoles in the string cancel each other and the mechanical action of the string is equivalent to two opposing forces $\pm P$ placed at $\pm N/2$. Therefore the string effectively acts like one dipole of total strength NP and the asymptotic potential decays with the dipolar power law $N/\pi x^3$. For $1 < x < N$, the string can be assumed to be infinite, but the discrete spacing between the dipoles can still be neglected. Then we can use the analogy to the electrostatic problem of an infinite, homogeneously charged line. Using Gauss' law and the fact that the force density vanishes gives that now the potential $W^{\parallel}$ has to be constant. The height of this plateau is fixed by the boundary conditions, that is, in our case by matching it to the large distance regime at $x \sim N$; therefore $W^{\parallel} \sim 1/N^2$. For $x \approx 1$, the finite spacing between the dipoles becomes relevant and the exponential decay $8\pi e^{-2\pi x}/\sqrt{x}$ predicted by Eq. (4) becomes valid. Finally, for $x < 1$ the interaction with the string is dominated by interactions with the closest dipole in the string and $W^{\parallel}$ crosses over to the dipolar power law $1/\pi x^3$. Figure 2 demonstrates the nice agreement between this scaling analysis and the full numerical result. While these four scaling regimes are valid in general, the exact details are very sensitive to dipole orientation, offset y and Poisson ratio ν. In particular, variations in ν can qualitatively alter the interactions, especially for $x < 1$, as demonstrated in the inset of Fig. 2 for an infinite string. In general, for an infinite string the large distance regime and the height of the plateau vanish, and we are left with the exponential decay derived above.

String formation is also known for passive particles, most prominently for electric dipoles [14,15]. The short-ranged nature of the effective interaction between strings due to screening inside the string is well known in this case [13,16,17], but to our knowledge has not been discussed before for force dipoles. It has several important implications for cellular structure formation. First, it suggests that long-ranged effects do not dominate structure formation at particle densities sufficiently large as to allow formation of strings of aligned dipoles. Second, for high particle densities the strong dependence of the string-string interaction on ν suggests that structural changes might occur as a function of Poisson ratio.

In order to address these issues, we used Monte Carlo simulations to study cellular structure formation on elastic substrates as a function of reduced cell density ρ and Poisson ratio ν. Because cells are supposed to interact only elastically, a circular exclusion zone was attributed to each cell and positional degrees of freedom were fixed at random, thus avoiding cell-cell contact. Experimentally, this situation might be realized by confining cells to adhesive islands created by microcontact printing on elastic substrates. We then relaxed the orientational degrees of freedom using a Gibbs ensemble on W with a small finite

effective temperature, which can be interpreted as an stochastic element in cellular decision making. Similar procedures have been used before for modeling cellular structure formation [18]. Based on our simulations we predict three different phases. At low density, we always find many short strings with little correlation. No global order appears, except when an external field is applied. Therefore this phase might be termed *paraelastic*. Presumably due to the screening effects described above, this globally disordered phase is stable up to relatively high densities. At high density and small values of the Poisson ratio ν, spontaneous polarization occurs; that is, the medium is contracted unidirectionally. This situation is reminiscent of certain pathological situations when wound contraction deteriorates into uncontrolled skin contraction (*contracture*). The corresponding phase of aligned strings might be termed *ferroelastic* and is characterized by a nonvanishing nematic order parameter S. As ν is increased at high cell density, the nematic order parameter vanishes again for $\nu_c = 0.32$; that is, the systems becomes macroscopically isotropic again, with a local structure which is ringlike rather than stringlike. This phase results from the Poisson effect and might be termed *antiferroelastic*. In Fig. 3, we show typical configurations and the phase transition line to the ferroelastic phase as measured in simulations by setting $S = 0.4$.

The important role of the Poisson ratio for cellular structure formation can also be demonstrated for regular arrangements of force dipoles. Figure 4 shows six candidate structures identified by Monte Carlo simulations for dipoles on square and hexagonal lattices. To identify optimal structures we calculate the interaction per particle by evaluating the corresponding lattice sums. For this purpose, we decompose the structures into A and B sublattices
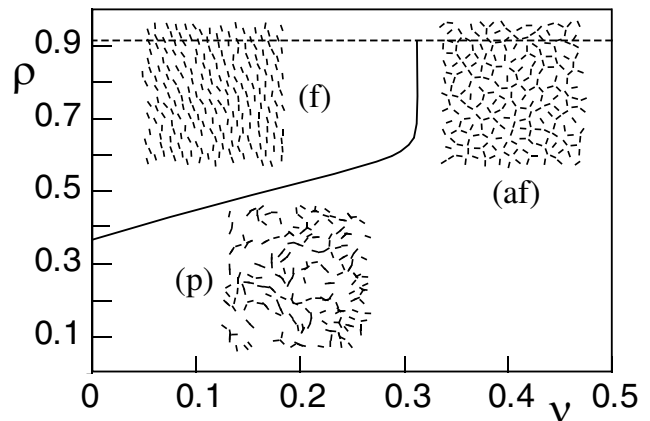

FIG. 3. Phase diagram for positionally disordered cells. At low cell density, an orientationally disordered (*paraelastic*) phase (p) prevails. At high cell density, orientational order sets in, with a nematic stringlike (*ferroelastic*) phase (f) at low values of Poisson ratio ν and a isotropic ringlike (*antiferroelastic*) phase (af) at large values of ν. Because we are in two dimensions, $\rho \leq 0.907$.
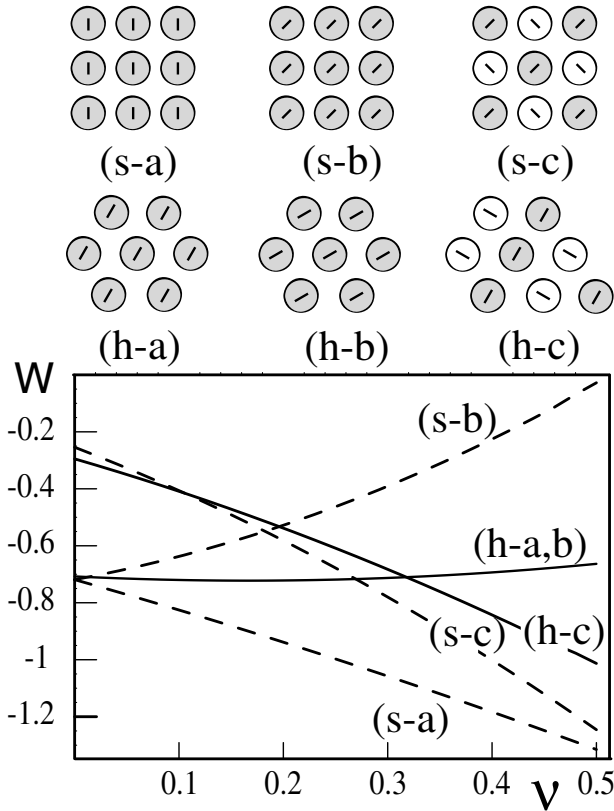
FIG. 4.   Structure formation of cells positioned on square (s) and hexagonal (h) lattices. Elastic interactions result in a competition between ferroelastic (a,b) and antiferroelastic structures (c) as a function of Poisson ratio ν and lattice geometry.

of parallel strings, as indicated by gray and white colors. The main contribution to W originates from interactions within a string and is given by $-2\zeta(3)(1 + \nu)$, where $\zeta(z)$ is the Riemann zeta function with $\zeta(3) \approx 1.29$. Because the interaction with adjacent strings decays exponentially as shown by Eq. (4), the interactions with adjacent strings are dominated by interactions with the nearest neighbor strings and the lattice sums converge quickly. The plots in Fig. 4 show that on hexagonal lattices, a phase transition from a ferroelastic (h-a,b) to an antiferroelastic structure (h-c) occurs at $\nu_c = 0.32$. On square lattices, W decreases strongly with ν for the antiferroelastic structure (s-c). However, here lattice geometry stabilizes the ferroelastic phase (s-a) over the whole range of ν, such that the ferro-antiferroelastic transition does not occur. This finding also implies that on substrates with $\nu \approx 0.4$ cellular structures might be switched between ferroelastic and antiferroelastic phases simply by varying the geometry of cell positioning.

In summary, we have shown that elastic interactions of cells lead to surprising and nontrivial structure formation as a function of cell density and Poisson ratio. Elastic substrates appear to be the ideal experimental systems to test our predictions since they allow us to focus on the

mechanical aspects of the environment in cell organization. In traditional systems like polymer gels made from poly-acrylamide or polydimethylsiloxane, the Poisson ratio usually is close to $1/2$. In order to test our predictions, novel polymer gels for cell culture are needed which allow us to tune the value of the Poisson ratio. The typical physiological environment of tissue cells are the hydrated polymer networks of the extracellular matrix and future work has to show how our results carry over to this situation. In particular more details of the cellular decision making process have to be included in this case. It is important to note that the Poisson ratio of a dehydrated polymer network can be much smaller than the one of a macroscopic region of a fully hydrated gel. One therefore might expect that the effective Poisson ratio relevant for cellular structure formation in hydrogels depends on the way water moves within the filamentous structure and therefore on the as yet unknown spatial and temporal scales on which cells probe this mechanical environment.

[1] T. Vicsek, A. Czirok, E. Ben-Jacob, I. Cohen, and O. Shochet, Phys. Rev. Lett. **75**, 1226 (1995).
[2] F. Schweitzer, W. Ebeling, and B. Tilch, Phys. Rev. Lett. **80**, 5044 (1998).
[3] Y. Hatwalne, S. Ramaswamy, M. Rao, and R. A. Simha, Phys. Rev. Lett. **92**, 118101 (2004).
[4] I. B. Bischofs and U. S. Schwarz, Proc. Natl. Acad. Sci. U.S.A. **100**, 9274 (2003).
[5] I. B. Bischofs, S. A. Safran, and U. S. Schwarz, Phys. Rev. E **69**, 021911 (2004).
[6] H. Wagner and H. Horner, Adv. Phys. **23**, 587 (1974).
[7] U. S. Schwarz and S. A. Safran, Phys. Rev. Lett. **88**, 048102 (2002).
[8] J.-B. Manneville, P. Bassereau, S. Ramaswamy, and J. Prost, Phys. Rev. E **64**, 021908 (2001).
[9] M. Dembo and Y.-L. Wang, Biophys. J. **76**, 2307 (1999).
[10] U. S. Schwarz, N. Q. Balaban, D. Riveline, A. Bershadsky, B. Geiger, and S. A. Safran, Biophys. J. **83**, 1380 (2002).
[11] S. Vanni, B. C. Lagerholm, C. Otey, D. L. Taylor, and F. Lanni, Biophys. J. **84**, 2715 (2003).
[12] A. J. Engler, M. A. Griffin, S. Sen, C. G. Bonnemann, H. L. Sweeney, and D. Discher, J. Cell Biol. **166**, 877 (2004).
[13] P. B. Allen, J. Chem. Phys. **120**, 2951 (2004).
[14] P. G. de Gennes and P. A. Pincus, Phys. Kondens. Mater. **11**, 189 (1970).
[15] T. Tlusty and S. A. Safran, Science **290**, 1328 (2000).
[16] E. Madelung, Phys. Z. **XIX**, 524 (1918).
[17] R. Tao and J. M. Sun, Phys. Rev. Lett. **67**, 398 (1991).
[18] D. A. Beysens, G. Forgacs, and J. A. Glazier, Proc. Natl. Acad. Sci. U.S.A. **97**, 9467 (2000).